Journal of Particle Science and Technology 7 (2) (2021) 83-98

Ministry of Science, Research & Technology
Iranian Research Organization for Science and Technology

Journal of PARTiCLE Science & Technology

JPST
https://jpst.irost.ir

Review article

Cyclone separator theories to predict performance and flow characteristics

Sakura G. Bogodage[1,*], Andrew Y. T. Leung[2]

[1] *Department of Civil and Environmental Technology, Faculty of Technology, University of Sri Jayewardenepura, Sri Lanka*
[2] *Caritas Institute of Higher Education, Hong Kong SAR, China*

HIGHLIGHTS

- Practical analyses to evaluate cyclone designs are cost and time exclusive.
- Limited literature is available to analyse the cyclone performance theoretically.
- Selected theories were studied based on the data from the literature.
- Theories by Muschelknautz and Shepherd and Lapple were partially compatible.
- Particle-particle-wall interactions and frictions should be analysed further to bring the theories real.

GRAPHICAL ABSTRACT

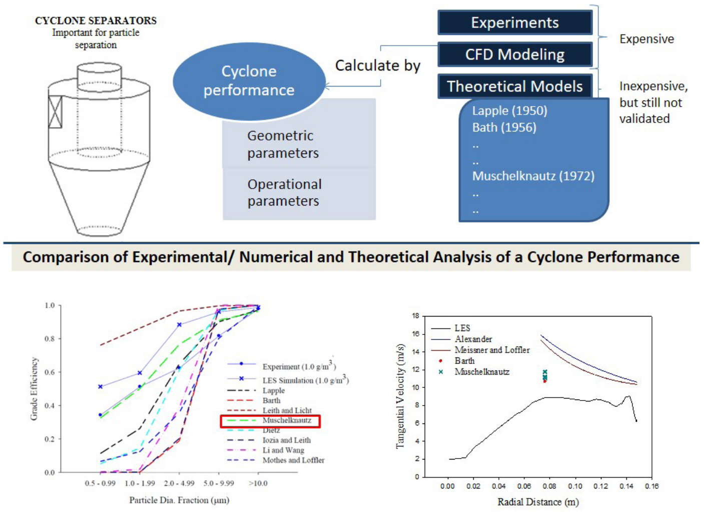

ARTICLE INFO

Article history:
Received 17 April 2022
Revised 2 June 2022
Accepted 2 June 2022

Keywords:
Cyclone separator theories
Collection efficiency
Pressure drop
Flow pattern
Particle flow

ABSTRACT

Several theoretical approaches for predicting performance parameters (collection efficiency, pressure drop, and velocities) of cyclone separators have been developed due to their extensive use in particle handling industries. Expensive and time-consuming experiments to analyze the swirling flow inside the cyclone separators could be avoided with reliable theoretical approaches. However, there are only a limited number of cyclone theory evaluations in the literature. This study investigated the accuracy of cyclone theories by comparing experimental and numerical data at a particle loading rate of 1.0 g.m^{-3} operating at 5 and 10 m.s^{-1}. General agreements between the theories were revealed by Muschelknautz's theory for collection efficiency and Shepherd and Lapple's theory for pressure variations at low solid loading conditions; disagreements were found to be due to the theories' insensitivity to influences from the particle phase and the frictional wall effect inside cyclone separators.

* *Corresponding author: Tel.: +9476-7050429 ; Fax: +9411-2801604 ; E-mail address: sakurabogoda@sjp.ac.lk*
DOI:10.22104/JPST.2022.5608.1207

1. Introduction

Cyclone separators are popular in particle handling industries because of their higher particle removal capability as well as their economic feasibility, ease of maintenance, and ability to operate in different environmental conditions. Ongoing experimental and numerical investigations have continued to improve cyclone separator's performance parameters, i.e., collection efficiency and pressure drop, as well as theoretical designs to predict cyclone performances. Assumptions common to all available theories are: 1) particles are spherical, 2) the particle motions are not influenced by neighbouring particles, 3) Stokes's law governs the radial force on particles, and 4) the gas radial velocity is zero [1]. The theoretical prediction of cyclone performance is vital for cyclone and plant design purposes, and even though all theories share the assumptions above, all theoretical models are also based on different assumptions of turbulence in cyclone flow and consider different specific geometric or operational conditions. Hence, the validity of a selected theory's experimental or numerical results cannot be predicted.

Early cyclone theory literature mainly consists of studies comparing cyclone theories with experimental or numerical results; however, comparisons are less common in later studies or the industry. Moreover, theories developed to predict cyclone performance are primarily related to the turbulence flow region of industrial-scale cyclone separators, and they have not been successful in predicting the performance of small cyclones [2].

In the present study, the most commonly used theories were analyzed by considering experimental and numerical data of the turbulence flow region of industrial-scale cyclone separators from Bogodage and Leung [3,4]. The selected particle loading rate was 1.0 g.m^{-3} at two inlet velocities, 5 and 10 m.s^{-1} [3]. The numerical data were taken from the numerical simulations done by Bogodage and Leung [4], and based on the same experimental conditions. Large Eddy Simulation (LES) was applied to model the particle-laden flow by considering one-way coupling conditions. However, since most of the available cyclone separator theories were based on cyclone separators with slot type inlets, circular type inlet data from Bogodage and Leung [3,4] was also considered as a rectangular type representing a similar cross-sectional area.

The present study reviewed the available cyclone theories and used experimental data [3] to obtain each theory's relevant collection efficiencies and pressure drops results. Also, numerical data from velocity profiles [4] were analyzed using the results from developed cyclone theories in the literature.

2. Collection Efficiency

Table 1 lists the theories used to calculate the collection efficiency of cyclone separators taken from the literature. These theories are briefly described in the following sections.

2.1. Lapple model

Lapple derived equations for cyclone collection efficiency (Eqs. (1) and (2)) based on the cut size diameter by applying the force balance theory, which assumes that the particles entering the cyclone separator are evenly distributed across the inlet opening, and those particles that travel from the inlet half-width to the wall during the processing time in the cyclone separator are collected with 50% efficiency [5]. Later, Theodore and

Table 1. Theoretical formulas of different collection models in the literature.

Modle	Equation(s)	
	$d_{50} = \sqrt{\dfrac{9\mu b}{2\pi\rho_p v_{in} N}}$	1
Lapple	$\eta_x = \dfrac{1}{1+\left(\dfrac{d_{50}}{d_x}\right)^2}$	2
	(proposed by Theodore and Paola [6])	

Bart	$d_{50} = \sqrt{\frac{9\mu Q}{\pi\rho_p v_{\theta cs}^2 h^*}}$	3
	$h^* = \begin{cases} H - S & if\ D_e < B \\ \frac{(H-h)(D-D_e)}{(D-B)} + (h-s) & if\ D_e > B \end{cases}$	4
	$v_{\theta cs} = v_x \left(\frac{0.5\pi D_e (D-b)}{2ab\alpha + h^*(D-b) f \pi}\right)$	5
	$\alpha = 1 - 1.2(\frac{b}{D})$	6
	$\eta_x = \frac{1}{1+\left(\frac{U_{ts}}{U_{ts}^*}\right)^{-3.2}}$	7
	$U_{ts}^* = \frac{Qg}{2\pi h^* v_{\theta cs}^2}$	8
	$\frac{U_{ts}}{U_{ts}^*} = \frac{\pi h^* v_{\theta cs}^2 \rho_p d_x^2}{9\mu Q}$	9
Leith and Licht	$\eta_x = 1 - \exp\left[-2\left(\frac{C\rho_p d_x^2 v_{in}^2 (n+1)}{18\mu D}\right)^{\frac{0.5}{(n+1)}}\right]$	10
	(*n* is calculated from Eq.64)	
	$c = \frac{\pi D^2}{ab}\left[2\left(1-\left(\frac{D_e}{D}\right)^2\right)\left(\left(\frac{S}{D}\right)-\left(\frac{\alpha}{D}\right)\right)+\frac{1}{3}(S+\iota-h)\left(1+\left(\frac{d_c}{D}\right)\right)+\left(\frac{d_c}{D}\right)^2+\left(\frac{h}{D}\right)-\left(\frac{D_e^2}{D}\right)\left(\frac{\iota}{D}\right)-\left(\frac{S}{D}\right)\right]$	11
	$d_c = D - \left(\frac{(D-B)(S+\iota-h)}{(H-h)}\right)$	12
	$\iota = \min\left\{(H-S), 2.3D_e\sqrt[3]{\left(\frac{D^2}{ab}\right)}\right\}$	13
Muschelknautz	$\eta = \sum_{i=1}^{N} \eta_i \times \Delta MF_i$	14
	$C_{0L} = \frac{f' D_m \mu}{2(1-\frac{D_e}{D})\rho_p d_{med}^2 v_{\theta m}}$	15
	$D_m = \sqrt{DD_e}, f' = 0.005(13\sqrt{C_0}), v_{\theta m}$	16
	$\eta_x = \frac{1}{1+\left(\frac{d_{50}}{d_x}\right)^m}$	17
	$d_{50} = d_{fact}\sqrt{\frac{18\mu(0.9Q)}{2\pi(\rho_p-\rho_g)}v_{\theta CS}(H-S)}$	18

	$\eta_x = 1-\left(K_0-\sqrt{K_1^2+K_2}\right)\exp\left(\frac{-\pi D U_{pw}\left(S-\frac{\alpha}{2}\right)}{Q}\right)$	19
	$\left.\begin{aligned} K_0 &= \frac{D_e U_{pw} + D\,U_{pw} + D_e W_{r0}}{2D_e U_{pe}} \\ K_1 &= \frac{D_e U_{pw} + D\,U_{pw} + D_e W_{r0}}{2D_e U_{pe}} \\ K_1 &= \frac{D_e U_{pw}}{D_e U_{pe}} \end{aligned}\right\}$	20
Dietz	$U_{pw} = \frac{\rho_p d_x^2 \nu^2_{\theta m}}{9\mu D}, U_{pv} = \frac{\rho_p d_x^2 \nu^2_{\theta e}}{9\mu D_e}, W_{r0} = \frac{Q}{\pi D_e \iota}$	21
	$\nu_\theta(r) = \nu_{\theta w}\,(\frac{D}{2r})^m, (0.5 < m < 1.0)$	22
	$\iota = \min\left\{H-S, 7.3\frac{D_e}{2}\sqrt[3]{\left(\frac{D^2}{4ab}\right)}\right\}$	23
Dirgo and Leith	$\eta_x = \frac{1}{1+\left(\frac{d_{50}}{d_x}\right)^{6.4}}$	24
	$\eta_x = 1-\frac{C_4(S)}{C_{0x}}$	25
	$C_4(S) = K_1\left(\frac{m_1-A}{B}\right)b$	26
	$K_1 = C_{0x}\exp\left(-\frac{2\pi R_{eq} U'_{tR_{eq}}(S-\frac{\alpha}{2})}{Q}\right)$	27
	$m_1 = \left(\frac{A+D}{2}\right)+\sqrt{\left(\frac{A+D}{2}\right)^2 - AD + BC}$	28
	$U'_{t(r)} = \frac{d_x^2 \rho_p \nu_\theta^2}{18\mu r}$	29
	$At\ r = R_{eq},\ U'_{t(r)} = U'_{tR_{eq}}\ and\ at\ r = R_{e,},\ U'_{t(r)} = U'_{tR_e}$	30
Mothes and Loffler	$R_{eq} = \sqrt{\frac{V_{Cyclone}}{\pi H}}$	31
	$\nu_{rCS} = \frac{Q}{\pi D_e (H-S)}$	32
	$When\ U'_{tR_e} > u_{rCS}$,	33
	$A = \frac{2\pi R_{eq} U'_{tR_{eq}}(H-S)}{Q} + \frac{2\pi R_e D(H-S)}{Q(R_{eq}-R_e)} - 1$	
	$B = \frac{2\pi R_e D(H-S)}{Q(R_{eq}-R_e)} - \frac{2\pi R_e (U'_{tR_{eq}} - \nu_{rCS})(H-S)}{Q}$	
	$C = \frac{2\pi R_e D(H-S)}{Q(R_{eq}-R_e)}$	
	$D = B-1$	

$$When\ U'_{tR_e} \le v_{rCS}\ ,$$ 34

$$A = \frac{2\pi R_{eq} U'_{tR_{eq}}(H-S)}{Q} + \frac{2\pi R_e D(H-S)}{Q(R_{eq}-R_e)} - \frac{2\pi R_e (U'_{tR_{eq}} - v_{rCS})(H-S)}{Q} - 1$$

$$B = \frac{2\pi R_e D(H-S)}{Q(R_{eq}-R_e)}$$

$$C = \frac{2\pi R_e D(H-S)}{Q(R_{eq}-R_e)} - \frac{2\pi R_e (U_{tR_{eq}} - v_{rCS})(H-S)}{Q}$$

$$D = B - 1$$

$$\eta = \frac{\int_0^\infty m_{in}\eta dd_x}{\int_0^\infty m_{in} dd_x}$$ 35

Iozia and Leith

Modified Barth method for v_t and h^*;

$$d_{50} = \sqrt{\frac{9\mu Q}{\pi\rho_p v_t^2 h^*}}$$ 36

$$v_t = 6.1\ v_i \left(\frac{ab}{D^2}\right)^{0.61} \left(\frac{D_e}{D}\right)^{-0.74} \left(\frac{H}{D}\right)^{-0.33}$$ 37

$$h^* = \begin{cases} H-S & if\ \ d_c < B \\ (H-S) - \dfrac{(H-h)}{((\frac{D}{B})-1)}\left(\left(\dfrac{d_c}{B}\right)-1\right) & if\ \ d_c > B \end{cases}$$ 38

$$d_c = 0.47D\left(\frac{ab}{D^2}\right)^{-0.26}\left(\frac{D_e}{D}\right)^{1.4}$$ 39

$$\eta_x = \frac{1}{1+\left(\dfrac{d_{50}}{d_x}\right)^{-3.2}}$$ 40

Li and Wang

$$\eta_x = 1 - \exp(-\lambda\theta_1)$$ 41

$$\theta_1 = \frac{2\pi(S+\iota)}{\alpha}$$ 42

$$\iota = \begin{cases} 2.3 D_e \sqrt[3]{\left(\dfrac{D^2}{ab}\right)} & if\ \ \iota < (H-S) \\ (H-S) & if\ \ \iota > (H-S) \end{cases}$$ 43

$$\lambda = \frac{(1-\alpha)Kw_p}{(\frac{D_r D^n}{2})},\quad when\ w_p(r)\ at\ \frac{D}{2}$$ 44

$$D_r = 0.052\left(\frac{D-D_e}{2}\right)v_{in}\sqrt{\frac{f}{8}},\quad assumed\ f = 0.02$$ 45

$$K = \frac{(1-n)(\rho_p-\rho_g)d_x^2 Q}{18\mu b\left(\dfrac{D^{n-1}}{2} - \dfrac{D_e^{\,n-1}}{2}\right)}$$ 46

$$w_p(r) = \frac{d_x^2(\rho_p-\rho_g)v_\theta(r)^2}{18\mu r}$$ 47

$$v_\theta(r) = \frac{(1-n)Q}{b\left(\dfrac{D^{n-1}}{2} - \dfrac{D_e^{\,n-1}}{2}\right)r^n}$$ 48

(*n* is calculated from Eq. (64))

Paola derived a graphical representative formula of the Lapple model [6].

Comparing the experimental results of Dirgo and Leith, who investigated collection efficiencies of a Stairmand high-efficiency cyclone with a diameter of 0.305 m at velocity conditions of 5 to 25 $m.s^{-1}$ with a solid loading rate up to 0.05 $g.m^{-3}$ [7], it is shown that Lapple's theory has underestimated collection efficiencies of larger particles and overestimated fine particles by owing flatter shape for grade efficiency curves. However, Lapple introduced a parameter called the number of revolutions, which can be adjusted between theoretical predictions and results by considering the experimental cut size diameter [5]. Lapple determined this value was 5 [5], but from Dirgo and Leith's experiments [7] found the value ranged from 10 to 25 as the inlet velocity increased. This theory's predictive value is limited as the results must be initially known. Jolius *et al*. model showed good agreement with experimental data available in the literature and with Lapple's model, but only for cyclone efficiencies under high temperature and high-pressure conditions [8].

2.2. Barth model

Barth derived another collection efficiency representation based on the diameter of the particle cut size by considering the balance between the centrifugal force and the drag force and calculating the terminal settling velocity for static particles [9]. The collection efficiency for any particle size is determined by the static particle's settling velocity to terminal settling velocity ratio. Governing equations of this theory are given in Eqs. (3)-(9). The Barth model has been proven to be an accurate model that needs further analysis, i.e., comparing its experimental results to Griffiths and Boysan [2] and Xiang *et al*. [10].

2.3. Leith and Licht model

Leith and Licht developed the first theory to predict cyclone collection efficiency in 1972; their theory recognized the inherent nature of flow and average resident times of the particles within the cyclone separator [11]. In this theory, the term *efficiency* was derived from the resident time of particles with deterministically calculated particle trajectories. The basic model equations are given in Eqs. (10)-(13). However, this theory is based on assumptions of uniform mixing of gas and particles at every cross-section and progressively cleaning approaching the exit, which means that the back-mixing of particles between two vortices in a cyclone separator is ignored in the calculations.

Nevertheless, many studies have proven that there is a concentration gradient in the radial direction of cyclones separators [12-14]. Also, there is a contradiction between theory and assumption as deterministic particle trajectories contradict the complete mixing of particles. Dietz stated that applying average residence time in calculations will effectively lower the collection efficiencies, and as a result, this theory should over-predict the collection [15]. Conversely, Leith and Licht's theory agrees very well with the grade-efficiency curves determined experimentally by Stairmand [16], as shown by Leith and Mehta [17]. However, contradicting this agreement, Chan and Lippmann [18], Dirgo and Leith [7], Li and Wang [19], and Griffiths and Boysan [2] have shown that this theory does not match experimental grade efficiency curves and over-predicts the particle cut size diameter.

Clift *et al*. have re-derived Leith and Licht model equations to correct particle removal on walls and approached the typical S-shaped curves generally found by many other researchers [20]. However, Clift's derivations also used the internal volume of the cyclone separator from Dacnkwerts without considering the inlet and outlet configurations, thus under-predicted the calculated particle residence time [21]. Moreover, Clift *et al*.'s [20] re-derived equations agree well with the experimental observations of Dirgo and Leith [7] but not those of Xiang *et al*. [10].

2.4. Muschelknautz model

The theory developed by Muschelknautz *et al*. improves Barth's theory by considering the effects of the particle load, the wall roughness, the secondary flow, and the change in particle size distribution within the body on the collection efficiency and the pressure loss [22,23]. This theory may be the most practical method for modelling cyclone separators at present [24]. This model is based on the *critical load* phenomena, which express the number of solids carried in a turbulent suspension. The main derivative equations are listed in Eqs. (14)-(18). However, considering the experimental investigations by Hoffmann *et al*., this method was not accurate in terms of critical loading [25].

2.5. Dietz model

Dietz [15] derived another theoretical model to predict the collection efficiency of cyclone separators (Eqs. (19)-(23)) by correcting Leith and Licht's [11] theory based on uniform mixing of particles and average residence time. He divided cyclone volume into three flow regions based on experimental observations by Linden [26], 1) the entry region, 2) the annular region, and 3) the core region, and considered particle interchange within the annular and core regions neglected by previous models. However, Dietz also assumed that turbulence produces a uniform radial concentration profile of particles within each region, similar to Leith and Licht's [11] theory, and neglected the axial back-mixing (re-entrainment) particles. Dietz's theory [15] obtained a satisfactory agreement with the experimental data by Stairmand [16]. However, Clift *et al*. [20] exposed some flaws in this theory related to the implied discontinuities of particles across the boundary between the annular and core regions, which is physically unrealistic. Additionally, Clift *et al*. stated that any satisfactory agreement of this theory with available experimental data is probably more incidental than a necessary consequence of the formulation of the model [20].

2.6. Dirgo and Leith model

Dirgo and Leith modified the Barth equation for the terminal velocity ratios by quadrupling it to match their experimental values and found a simple expression for Barth's plot of the collection efficiency versus the ratio (Eq. (24)) [7].

2.7. Mothes and Löffler model

As an alternative to Muschelknautz's [22] critical loading concept, Mothes and Löffler [27] modified Dietz's [15] theory by including an extra flow region close to the dust exit at the bottom of the cyclone to express the effect of dust re-entrainment. Based on particle agglomeration, they calculated the impact probability and sticking probability and accounted for turbulent diffusivity in both the annular and core regions. Compared to the Dietz model [15], this approach avoids the discontinuity of particles and analyzes particle trajectories by superimposing a diffusive motion (applicable with the shape of a grade-efficiency curve) with a deterministic mean motion (which mainly describes the cut-size diameter, d_{50}) [28,29]. A large number of theoretical derivations of this model are given in Eqs. (25)-(35). An excellent agreement of this model with available experimental data has been illustrated by Clift *et al*. [20] and Bingtao *et al*. [30]. However, Clift *et al*. [20] also stated that the predictive capability of this model is hindered by the lack of estimations for the particle dispersion coefficient (i.e., the effective turbulent diffusivity).

2.8. Iozia and Leith model

Iozia and Leith [31] proposed different equations (Eqs. (360-(40)) for the Barth model to match their cyclone geometries experiments. These equations were related to tangential velocity, the height of the cylindrical core, and the cylinder's diameter at natural depth. They stated that this equation agreed with their experiments. Xiang *et al*. [10] also confirmed a more reasonable agreement between this theory and Barth's theory [9] than Leith and Licht [11]. Nevertheless, this contrasted with experimental results by Kim and Lee, as shown by Griffiths and Boysan [2].

2.9. Li and Wang model

Li and Wang [19] dropped the hypothesis of different flow regions within a cyclone but recognized the role of finite turbulent particle diffusivity in producing radial concentration gradients. This theory was derived by neglecting turbulent particle dispersion throughout the interior cyclone but maintaining the particle concentration gradient. At the same time, the particle concentration gradient at the walls was assumed to be zero but with finite turbulent diffusivity at the wall. This model includes particle bounce or re-entrainment and turbulent diffusion at the cyclone wall. Mathematical equations based on this model are shown in Eqs. (41)-(48). The authors have validated the best prediction capability of their model by considering experimental results in Dirgo and Leith [7] and other theoretical models from the literature. However, Kim and Lee [32] later stated that the theory was questionable because of an abnormally high tangential velocity, unrealistic wall boundary conditions, and the violation of the conservation of particles.

Numerical evaluations of theoretical models by Jolius *et al*. [8] found that Li and Wang's [19] predictions agreed better with experimental investigations by Kim and Lee [33], Dirgo and Leith [7], and Ray *et al*. [34] than other collection efficiency models [5,31].

3. Pressure drop

Theoretical models for calculating pressure drop are still being developed, and they all have limitations relevant to the considered experimental conditions. Several popular theories are given in Table 2.

3.1. Shepherd and Lapple model

Shepherd and Lapple's [35] pressure drop expression (Eq. (49)) is an empirical model and can be considered the simplest model that only integrates the dimension of the gas inlet and outlet. Therefore, the ability to compare different geometries and operational conditions is unavailable in the Shepherd and Lapple model. Nevertheless, this theory showed accurate data for the evaluated correlation coefficients by Leith and Mehta [17].

3.2. Stairmand model

Stairmand [36] proposed another theory by first developing velocity distribution theories from a moment of momentum balance in the cyclone separator and then estimating the pressure drop by incorporating the entrance and exit losses and static pressure loss inside the vortex. The Stairmand model was condensed by Iozia and Leith [31] by calculating correlation coefficients (Eqs. (50)-(51)). Leith and Mehta [17] showed that this method is suitable for prediction due to having the exact correlation value as the Shepherd and Lapple model.

3.3. Barth model

Barth [9] proposed his theory of pressure drop in cyclone separators for given pressure losses at the inlet, cyclone body, and vortex finder. However, the author stated that the calculations could safely ignore the inlet pressure loss. The pressure loss inside the cyclone body was accounted for by the loss of swirl velocity at the imagined friction surface (Eq. (52)). The friction factor was accounted for in the effect of solid loading in this

Table 2. Theoretical formulas of different models in the literature related to pressure drop prediction.

Model	Equation(s)	
Shepherd and Lapple	$\Delta P = \frac{\rho_g v_{in}^2}{2}\left(\frac{16ab}{D_e^2}\right)$	49
Stairmand	$\Delta P = \frac{\rho_g v_e^2}{2}\left[1+2q^2\left(\frac{2(D-b)}{D_e}-1\right)+2\left(\frac{4ab}{\pi D_e^2}\right)^2\right]$	50
	$q = \frac{-\left(\frac{D_e}{2(D-b)}\right)^{0.5}+\left(\frac{D_e}{2(D-b)}+\frac{4A_R G}{ab}\right)^{0.5}}{\left(\frac{2A_R G}{ab}\right)}, (G = 0.005)$	51
Barth	$\Delta P_{body} = \frac{\rho_g v_e^2}{2}\frac{D_e}{D}\left[\frac{1}{\left(\frac{v_e}{v_{\theta CS}}-\frac{(H-S)}{0.5D_e}f\right)^2}-\left(\frac{v_{\theta CS}}{v_e}\right)^2\right]$	52
	$\Delta P_e = 0.5\rho_g v_e^2\left[\left(\frac{v_{\theta CS}}{v_e}\right)^2+K\left(\frac{v_{\theta CS}}{v_e}\right)^{\frac{4}{3}}\right]$	53
	$\Delta P_{tot} = \Delta P_{body} + \Delta P_e$	54
	$f = 0.005(1+3\sqrt{C_0})$	55
	$K = \begin{cases} 3.41 & \text{for vortex finders with rounded edges} \\ 4.40 & \text{for vortex finders with sharp edges} \end{cases}$	

	$\Delta P_{body} = \frac{f A_R \rho_g (v_{\theta w} v_{\theta CS})^{1.5}}{1.8Q}$	56
	$\Delta P_e = 0.5\rho_g v_e^2 \left[\left(\frac{v_{\theta CS}}{v_e}\right)^2 + K\left(\frac{v_{\theta CS}}{v_e}\right)^{\frac{4}{3}}\right]$	57
	$\Delta P_{acc} = (1+C_0)\frac{\rho_g (v_2^2 - v_1^2)}{2}$	58
Muschelknautz	$\Delta P_{tot} = \Delta P_{body} + \Delta P_e + \Delta P_{acc}$	59
	$f = f + 0.25\left(\frac{R}{R_e}\right)^{-0.625}\sqrt{\frac{\eta Fr_e \rho_g}{\rho_{str}}}$	60
	$K = \begin{cases} 3.41 & \textit{for vortex finders with rounded edges} \\ 4.40 & \textit{for vortex finders with sharp edges} \end{cases}$	
	(For more details refer Muschelknautz [22,23]).	
Casal and Martinez	$\Delta P = \frac{\rho_g v_{in}^2}{2}\left[3.33 + 11.3\left(\frac{ab}{D_e^2}\right)\right]$	61

model, which other theories have not presented. Barth stated the pressure drop in the vortex finder with a semi-empirical relationship (Eq. (53)). Leith and Mehta also showed the good prediction capacity of this model in their paper using correlations [17].

3.4. Muschelknautz method

Muschelknautz's method (Eqs. (56)-(60)) of pressure drop prediction is based on the pressure losses in the cyclone body (frictional wall loss) and the losses in the vortex core; the vortex finder contributed to the losses by particle loading and flow acceleration pressure loss [22,23]. By computing the loss due to the mass loading effect, the Barth equation (Eq. (57)) has been used for calculations relevant to Muschelknautz values.

3.5. Casal and Martinez model

The Casal and Martinez model [37] also proposed a simple empirical relationship (Eq. (61)) for pressure drop, incorporating inlet and outlet dimensions of the cyclone separator, which do not vary with other physical and operational conditions.

4. Fluid flow pattern

The cyclone flow pattern is made up of the distribution of axial, tangential, and radial velocities and is intended to predict particle separation. The most significant velocity component is the tangential velocity as it governs the particle separation process ,followed in importance by the axial and then radial velocities. The tangential velocity has been modeled in many works of literature. The models for tangential velocity prediction are listed in Table 3.

4.1. Alexander model

Alexander [38] was the first to introduce a theoretical model for the flow pattern in a cyclone separator (Eqs. (62)-(64)). He defined a purely empirical model by correlating the ratio of wall tangential velocity to mean velocity at the inlet, which is reasonable at high Reynolds numbers, and also defined the viscosity variation with the gas temperature by defining an exponent. This model only suits cyclone separators with smooth walls operating at low solid loading conditions [2]. This approach is flawed with regard to reality as it assumed that swirling velocity at the wall is equal to the inlet velocity regardless of the inlet shape. Patterson and Munz [39] found the tangential velocity predicted by this method had a good agreement at room temperature but not at higher temperatures and was also sensitive to geometric conditions. Bingtao *et al*. [30] also best matched the results from the Alexander model indicating the complex nature of the Vortex exponent, n, which depends on Reynolds number, cyclone design, and wall roughness.

4.2. Barth model

Barth's empirical model [40] is based on an imaginary cylindrical core that extends the vortex finder downward directly to the bottom of the cyclone along the same axis. The height and diameter of this extended section are and. This is the earliest model that incorporates the influence of wall friction and cyclone geometric parameters into tangential velocity components. The basic equations in this method are shown in Eqs. (65)-(68).

4.3. Muschelknautz method

Expanding on Barth's model, Muschelknautz [22,23] developed a much more realistic model to predict flow patterns inside a cyclone separator by considering wall friction and mass loading effects. Theoretical equations are shown in Eqs. (69)-(72).

4.4. Meissner and Löffler method

The Meissner and Löffler method [41] shown in Table

Table 3. Theoretical formulas of different models in the literature for predicting flow pattern in a cyclone separator.

Modle	Equation(s)	
Alexander	$v_\theta = v_{\theta CS}\left(\frac{R}{r}\right)^n$	62
	$\frac{v_{\theta w}}{v_{in}} = 2.15\left(\frac{A}{DD_e}\right)^n$	63
	$n = 1-(1-0.67D^{0.14})\left(\frac{T}{283}\right)^{0.3}$	64
Barth	$v_{\theta CS} = v_x\left(\frac{R_x R_{in}\pi}{ab\alpha + h^* R_{in}\pi f}\right)$	65
	$\alpha = 1-0.4\left(\frac{b}{D}\right)^{0.5}, R_{in} = R-\left(\frac{b}{2}\right)$	66
	$h^* = \begin{cases} H-S & D_e \le B \\ \frac{(H-S)(D-D_e)}{(D-B)}+(h-S), & D_e > B \end{cases}$	67
	$f = 0.02$	68
Muschelknautz	$v_{\theta CS} = \frac{v_{\theta w}}{R_e}\frac{R}{\left[1+\frac{f\, v_{\theta w} A_R\sqrt{\frac{R}{R_e}}}{2Q}\right]}$	69
	$v_{\theta w} = \frac{v_{in}R_{in}}{\alpha R}$ and $\xi = \frac{b}{R}$	70
	$\alpha = \frac{1}{\xi}\left(1-\sqrt{1+4\left[\left(\frac{\xi}{2}\right)^2-\frac{\xi}{2}\right]\sqrt{1-\frac{(1-\xi^2)(2\xi-\xi^2)}{1+C_0}}}\right)$	71
	$f = 0.005(1+3\sqrt{C_0})$	72

	$v_\theta(r) = 1 + \frac{v_{\theta w}}{\frac{r}{R}\left[\langle v_z\rangle\left(f_{tid}+\frac{f_{cone}}{\sin\in}\right)\left(1-\frac{r}{R}\right)\right]}$	73
	(To calculate $v_{\theta CS}$, insert $r= R_e$)	
	$\frac{v_{in}}{v^*_{\theta w}} = -0.204\frac{b}{R}+0.889$	74
Meissner and Löffler	$v_{\theta w} = \frac{\langle v_z\rangle}{f_{cy\,t}H^*_{cy\,t}}\left[\sqrt{\frac{1}{4}+f_{cy\,t}H^*_{cy\,t}\frac{v^*_{\theta w}}{\langle v_z\rangle}}-\frac{1}{2}\right]$	75
	$H^*_{cy\,t} = \frac{\alpha}{R}\left[\frac{-a\ \mathrm{rccos}(1-\frac{b}{R})}{2\pi}\right]+\frac{H_{cy\,t}}{R}$	76
	$\frac{0.0065 < f_{cy\,t}}{f_{tid}} / f_{cone<0.0075}$	

3 predicts the flow field based on the Momentum-of-momentum balance of the flow with Eqs. 73-76. This model was developed by dividing cyclone separator flow into vertical cylindrical elements and balancing the in and out of the momentum of momentum with the friction forces at the top and bottom of the cyclone separator, neglecting the wall friction of the cylindrical body. However, this model is also limited to predicting flow patterns of cyclone separators with slot type inlets and cylinder-on-cone designs. Also, it is only applicable in low mass loading conditions because this theory does not quantify the dust deposition effect on the wall friction factor. However, this model over-predicted the experimental data by Patterson and Munz [39] and Bingtao *et al*. [30].

5. Results and Discussion

5.1. Collection efficiency

Most available theories attempt to calculate cyclone efficiency related to particle size (grade efficiencies and cut-size diameters). The theoretical grade efficiency curves were calculated using theories by Lapple [5], Barth [9], Leith and Licht [11], Muschelknautz [22,42], Dietz [15], Iozia and Leith [43], Li and Wang [19] and Mothes and Loffler [44] and are shown in Fig. 1 for two considered inlet velocities.

Comparing experimental and LES simulation grade efficiency curves in Fig. 1 shows that the numerical results over-predict experimental results at a 10 $m.s^{-1}$ inlet velocity. In contrast, the numerical results at 5 $m.s^{-1}$ over-predict the particle range more than 5.0 µm while under-predicting particles smaller than 5.0 µm. However, the numerical results are due to particle agglomeration and re-entrainment, which were not considered in the modelling. Particle re-entrainment and agglomeration are well-known phenomena in cyclone separators [27,45] but are challenging to account for in modelling due to a lack of information. In addition, at high velocities, more particles are dragged by the flow to the cyclone bottom, where they collect at low velocities. As this study assumed that particles touching the cyclone bottom were collected, the numerical results at 10 $m.s^{-1}$ give higher collection efficiency. The agglomeration effect is more pronounced at low velocities due to the longer particle residence times. So, the particle agglomeration in cyclonic flow was higher at low velocities, with the impact of higher particle concentration zones near the walls and apex. In contrast to over-predicted grade efficiencies at 10 $m.s^{-1}$, the numerical results were underestimated at 5 $m.s^{-1}$ due to ignoring particle agglomeration.

Fig. 1 shows that all theories' theoretical grade efficiency curves followed the typical 'S-shaped' pattern by predicting low collection efficiencies for fine particles and higher efficiencies for coarse particles. However, flatter curves are shown for the theories of Leith and Licht, and Muschelknautz. The grade efficiency curves calculated by the theoretical predictions of Barth, Dietz, Iozia and Leith, and Li and Wang under-predict the experimental observations, especially for fine particles

(< 5.0 μm) at both velocities considered. At 10 $m.s^{-1}$ velocity, the computed grade efficiencies for coarse particles (5.0 - 10.0 μm) are also overestimated by the theories of Barth, Dietz, Iozia and Leith, and Li and Wang. At 5 $m.s^{-1}$, the calculated grade efficiencies generally agree with the experimental results, except for those of Dietz and Li and Wang.

The Leith theory is a modification of the Barth and Iozia theory obased on experimental data with different cyclone geometries. Both approaches consider the cyclone geometric properties and the inlet velocities but ignore the effects of particle loading and the geometry of the hoppers. However, Griffiths and Boysan [2] reported the superiority of Iozia and Leith's theory over Barth's theory compared to the experimental investigation by Dirgo and Leith [7]. Conversely, this study did not observe this improvement, as the two theories coincide. Dietz's theory generally follows Lapple's theory, but the values are less accurate. Although Dietz's theory is more realistic than theories by Lapple, Barth and Leith, and Licht, its accuracy is limited by the assumptions of uniform mixing of particles and average residence time. The theory developed by Li and Wang is known to be more practical because it includes the particle diffusivity that produces radial concentration gradients. Gimbun *et al*. [46] showed the best agreement with this theory occurred in the experimental grade efficiency curves by Dirgo and Leith [7] and Kim and Lee [32]. However, Li and Wang's theory fails to provide accurate results here. Another issue that arose in the present calculations in Li and Wang's theory was the value assumed for the coefficient of particle bounce or re-entrainment, α. This study defined it as zero to achieve the highest collection efficiencies, but this is unrealistic. However, the inapplicability of Li and Wang's theory in the present study may also be due to the high operating particle concentrations used by Dirgo and Leith [7] and Kim and Lee [32].

The Lapple method provides satisfactory results for the 2.0 - 10.0 μm particle range at two velocities but underestimates the finer fractions. This theory's parameter representing the number of turns, N, depends on a particular cyclone design and inlet velocity. Hence, the theory's dependence on N may influence the results, and the value of 12 is used in the present calculations. The theory of Mothes and Loffler calculated grade efficiencies for particles at 5.0 - 10.0 μm agrees with the experimental investigations at 10 $m.s^{-1}$ velocity. All of these theories agree with the experiments run with particles larger than 10.0 μm. At a 5 $m.s^{-1}$ velocity, the theoretical grade efficiencies are underestimated for the fine particle (< 5.0 μm) collection efficiencies but generally agree with particles larger than 5.0 μm. The highest deviations are shown from the theories of Mothes and Loffler and Li and Wang.

The theories of Barth, Li and Wang, and Mothes and Loffler account for the constant wall frictional effect. However, they do not fully reflect reality due to the significant dependency of the friction factor on particle loading rate. In addition, the constant turbulent diffusivity assumed by Mothes and Loffler is unrealistic.

The theory developed by Leith and Licht always gives the highest over-predicted grade efficiencies and shows a flatter curve than the standard 'S-shaped' pattern. This theory assumes uniform mixing of gas and particles at every axial cross-section and consequently provides different grade efficiency curves. Similar grade efficiency patterns for Leith and Licht's theory were also observed by Griffiths and Dirgo and Leith [7], Clift *et al*. [20], Boysan [2], and Kuo and Tsai [47].

Muschelknautz's theory is the only theory that considers the effects of particle loading calculations. However, grade efficiency curves of this theory indicate differences between the d_{fact} and values (defined by Muschelknautz) and the experimental values. The theory defined the d_{fact} in a range of 0.9 to 1.4, but the calculations based on the experimental results gave a range of 0.18 to 3.2. The theory defined the slope m as 2.0 to 7.0, but this study found it to be 0.18 to 1.8. Therefore, a careful review of the d_{fact} and values should be conducted to understand the accuracy of Muschelknautz's theory.

5.2. Pressure drop

The pressure drops were calculated using the theories of Stairmand [36], Barth [9], Shepherd and Lapple [35], Casal and Martinez [37], and Muschelknautz [22,42] and compared with the experimental and numerical values (Table 4).

Amongst these models, Stairmand and Barth developed their pressure drop equations by considering only the pressure losses at the inlet and outlet and the swirling loss at the cyclone body. However, these two models do not account for the substantial loading effect. The importance of solid loading in cyclone pressure drop estimation has been reported by many studies [48-51]. In practice, the pressure losses at the inlet and outlet are insufficient due to significant losses in the dust collection section. The dust collection section is vital in pressure drop reduction because sudden extraction, a swirling effect, and high particle concentration zones contribute to the pressure loss in this section. Thus, the overestimation of the theoretical pressure drops from these two models emphasizes the importance of these factors in theoretical approaches.

Pure empirical models developed by Shepherd and Lapple and Casal and Martinez supported a comprehensive analysis of the experimental data, ignoring operational conditions. They were only based on the cyclone inlet and outlet (vortex finder inlet). Regarding the pressure drop data in the present study, while the Casal and Martinez model over-predicted results, the Shepherd and Lapple model worked well. Shepherd and Lapple's theory performed best of the selected pressure drop theories, the reason behind its accuracy is uncertain but may be due to pressure drop sampling points in the experiment. In Bogodage and Leung's experiment [3], pressure drops were measured between the inlet and outlet, but the outlet was not located at the vortex finder. Therefore, the accuracy of the theoretical results in the Shepherd and Lapple model theoretical results was difficult to analyze. However, considering the similarity, general assumptions can be made. For example, the pressure drops due to sudden contractions in cyclone separators, and expansions at the natural inlet and outlet can alternate the swirling losses at the body.

The mechanistic theory developed by Muschelknautz also overestimates the experimental pressure drops even though it includes wall friction losses due to solid loading and losses in vortex core due to calculated pressure drops. The pressure drops calculated by this model shows the most significant overestimation of all the theories.

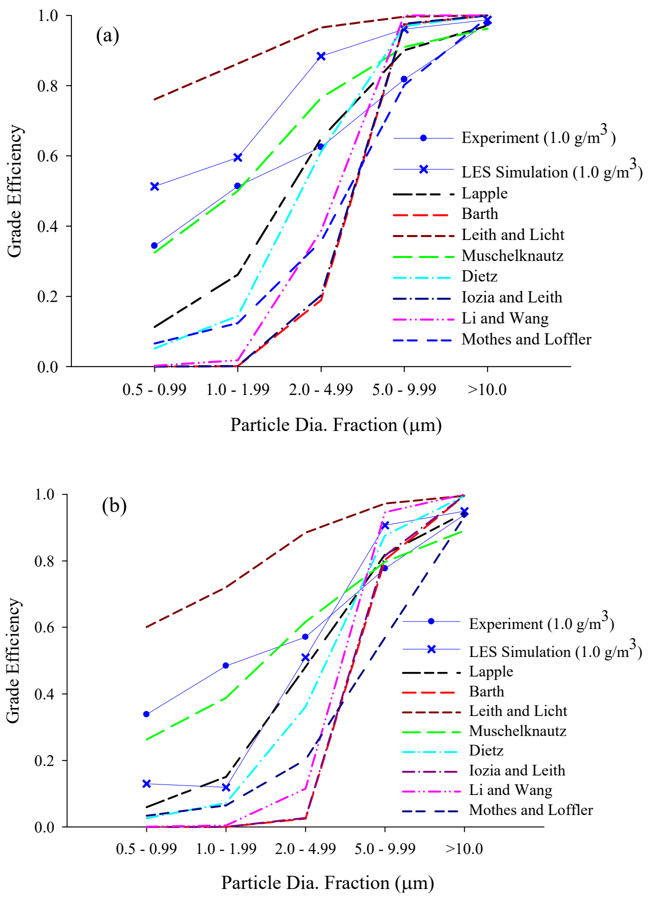

Fig. 1. Comparison of the theoretical grade efficiencies with the experimental [3] and numerical [2] investigations. (a) at 10 m.s^{-1} and (b) at 5 m.s^{-1}.

5.3. *Flow pattern in cyclone separators*

The tangential velocity component is the governing velocity in cyclone separator swirling flow. The theories developed by Alexander [38], Meissner and Löffler [41], Barth [9], and Muschelknautz [22,42] (summarized in Table 3) were used in this study to calculate the tangential velocity. Due to the unavailability of experimental velocities, only the numerical results were compared. Comparisons were only conducted for 10 m/s inlet velocity. The results are shown in Fig. 2.

The empirical theories developed by Alexander and Messner and Loffler can predict the tangential velocity field at the outer vortex. However, Fig. 2 shows these two methods overestimate the tangential velocity. And although Messner and Loffler's theory uses the wall friction factor, there were no apparent improvements. While both Barth and Muschelknautz's theories consider the tangential velocity at the control surface of the cyclone separator and the wall friction factor, they still over-predicted results compared to the numerical value.

The theoretical models for tangential velocity predictions cannot provide actual velocity fields, unlike the theoretical models used to foresee performance parameters. Derksen *et al*. [52], Qian e*t al*. [53], and Xue *et al*. [13] numerically investigated the reduction of velocity caused by the presence of solid particles. The present LES simulation applied a one-way coupling of particles so that the effect from the particle phase to the

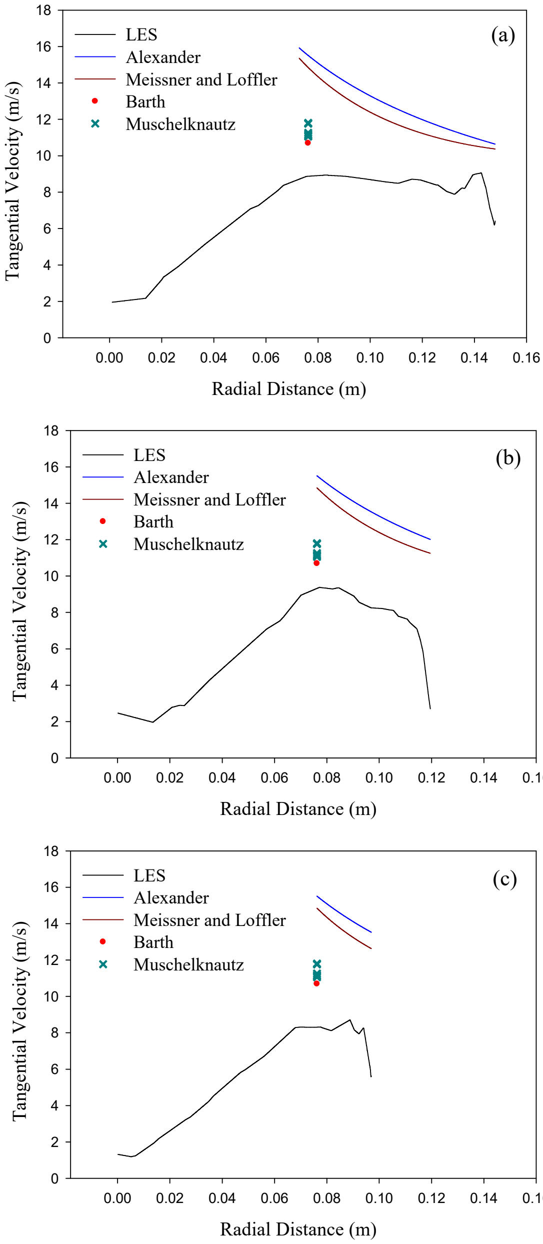

Fig. 2. Theoretical tangential velocities compared with numerical tangential velocities [2] (a) 0.075 m; (b) 0.2 m and (c) 0.3 m downward to the vortex finder inlet.

fluid phase was ignored. Therefore, the actual tangential velocity should be lower than the presented numerical values; so, again the theories did not match the actual values.

6. Conclusions

Theoretical explanations of the cyclone performance and flow characteristics are essential in designing high-efficiency cyclone separators. The selected theories were compared with experimental and numerical investigations to analyze their applicability. The following conclusions were derived from this study.

1. The theoretical models for calculating the collection efficiencies of cyclone separators were developed at low solid loading rates. Muschelknautz's theory provided results that generally agreed with the experimental results, although it was designed to analyze two variables, d_{fact} and , with more experimental data. The other theories always followed the 'S-shaped' grade efficiency curves that ignored the increase in fine particle collection due to particle agglomeration. In addition, the theories over-predicted the coarse particle ranges because they did not consider particle re-entrainment.
2. The pressure drop is an essential parameter of cyclone design regarding energy efficiency. Among the theories selected in this study, only the purely empirical model presented by Shepherd and Lapple accurately predicted the results. The accuracy of this theory could not be clarified due to the differences in the pressure drop measured points in the experiments.
3. Predicting theoretical flow patterns is difficult due to unknown influences from the particle phase and

Table 4. Experimental, numerical and theoretical pressure drops at two different inlet velocities.

Method	**Pressure drop (Pa)**	
	At 5 m.s^{-1}	**At 10 m.s^{-1}**
Experimental (at solid loading rate of 1.0 g.m^{-3})	37.30	157.05
Numerical (LES method) (at solid loading rate of 1.0 g.m^{-3})	43.8	198.74
Shepherd and Lapple	38.75	155.00
Stairmand	60.31	241.25
Barth	70.66	282.3
Casal and Martinez	54.36	217.47
Muschelknautz (at solid loading rate of 1.0 g.m^{-3})	136.91	336.25

the frictional wall effect at different zones inside the cyclone. Therefore, none of the selected theories accurately predicted the flow patterns, and all gave over-predicted results.

In summary, although it has been several decades since the first cyclone theories were developed, none of the existing theories provide satisfactory results. The key issues arise in the discrepancies of the theoretical predictions, which ignore particle agglomeration, particle re-entrainment, and the geometry of the dust collection section in derivations. In addition, the theories do not consider the variations in the wall friction coefficient and the turbulent diffusivity of particles at higher solid loading conditions. These are the main weaknesses of the selected theories relevant to this study.

Acknowledgement

The research was supported by the University Grant Committee of HKSAR, grant number GRF 115712.

References

[1] A.C. Hoffmann, L.E. Stein, Gas Cyclones and Swirl Tubes: Principles, Design, and Operation, 2nd ed., Springer Berlin Heidelberg, Germany, 2002.

[2] W. Griffiths, F. Boysan, Computational fluid dynamics (CFD) and empirical modelling of the performance of a number of cyclone samplers, J. Aerosol Sci. 27 (1996) 281-304.

[3] S.G. Bogodage, A. Leung, Improvements of the cyclone separator performance by down-comer tubes, J. Hazard. Mater. 311 (2016) 100-114.

[4] S.G. Bogodage, A.Y.T. Leung, CFD simulation of cyclone separators to reduce air pollution, Powder Technol. 286 (2015) 488-506.

[5] C.E. Lapple, Gravity and centrifugal separation, Am. Ind. Hyg. Assoc. Q. 11 (1950) 40-48.

[6] L. Theodore, V.D. Paola, Predicting cyclone efficiency, J. Air Pollut. Cont. Assoc. 30 (1980) 1132-1133.

[7] J. Dirgo, D. Leith, Cyclone collection efficiency: comparison of experimental results with theoretical predictions, Aerosol Sci. Tech. 4 (1985) 401-415.

[8] G. Jolius, L.A. Chuah, C. Thomas, T.S. Yaw, A. Fakhru'l-Razi, Evaluation on empirical models for the prediction of cyclone efficiency, 2006.

[9] W. Barth, Design and layout of the cyclone separator on the basis of new investigations, Brenn. Warme Kraft, 8 (1956) 1-9.

[10] R. Xiang, S. Park, K. Lee, Effects of cone dimension on cyclone performance, J. Aerosol Sci. 32 (2001) 549-561.

[11] D. Leith, L. W., The collection efficiency of cyclone type particle collectors. A new theoretical approach, presented at the AICHE Symposium Series, U.S.A., 1972.

[12] G. Wan, G. Sun, X. Xue, M. Shi, Solids concentration simulation of different size particles in a cyclone separator, Powder Technol. 183 (2008) 94-104.

[13] X. Xue, G. Sun, G. Wan, M. Shi, Numerical simulation of particle concentration in a gas cyclone separator, Petrol. Sci. 4 (2007) 76-83.

[14] H. Mothes, F. Löffler, Bewegung und abscheidung der partikeln im zyklon, Chem-Ing-Tech. 56 (1984) 714-715.

[15] P. Dietz, Collection efficiency of cyclone separators, AIChE J. 27 (1981) 888-892.

[16] C.J. Stairmand, The design and performance of cyclone separators, Trans. Instn. Chem. Eng. 29 (1951) 356-383.

[17] D. Leith, D. Mehta, Cyclone performance and design, Atmos. Environ. (1967), 7 (1973) 527-549.

[18] T. Chan, M. Lippmann, Particle collection efficiencies of air sampling cyclones: an empirical theory, Environ. Sci. Technol. 11 (1977) 377-382.

[19] L. Enliang, W. Yingmin, A new collection theory of cyclone separators, AIChE J. 35 (1989) 666-669.

[20] R. Clift, M. Ghadiri, A.C. Hoffman, A critique of two models for cyclone performance, AIChE J. 37 (1991) 285-289.

[21] P.V. Danckwerts, Continuous flow systems: distribution of residence times, Chem. Eng. Sci. 2 (1953) 1-13.

[22] E. Muschelknautz, V. Greif, Cyclones and other gas-solids separators, in Circulating Fluidized Beds, ed.: Springer, 1997, pp. 181-213.

[23] E. Muschelknautz, Die berechnung von zyklonabscheidern für gase, Chem-Ing-Tech. 44 (1972) 63-71.

[24] A.C. Hoffmann, L.E. Stein, P. Bradshaw, Gas cyclones and swirl tubes: principles, design and operation, Appl. Mech. Rev. 56 (2003) B28-B29.

[25] A. Hoffmannc, A. Van Santen, R. Allen, R. Clift, Effects of geometry and solid loading on the performance of gas cyclones, Powder Technol. 70 (1992) 83-91.

[26] A. Ter Linden, Investigations into cyclone dust collectors, Proceedings of the Institution of Mechanical Engineers, 160 (1949) 233-251.

[27] H. Mothe, F. Loffler, Prediction of Particle Removal in Cyclone Separator, Int. Chem. Eng. 28 (1988) 231-240.

[28] B. Zhao, Development of a new method for evaluating cyclone efficiency, Chem. Eng. Process. 44 (2005) 447-451.

[29] R.L. Salcedo, M.A. Coelho, Turbulent dispersion coefficients in cyclone flow: An empirical approach, Can. J. Chem. Eng. 77 (1999) 609-617.

[30] Zhao, Bingtao, Dongshen Wang, Yaxin Su, Hua-Lin Wang. Gas-particle cyclonic separation dynamics: modeling and characterization, Sep. Purif. Rev. 49 (2020) 112-142.

[31] D. L. Iozia, D. Leith, The logistic function and cyclone fractional efficiency, Aerosol Sci. Technol. 12 (1990) 598-606.

[32] J. Kim, K. Lee, Experimental study of particle collection by small cyclones, Aerosol Sci. Technol. 12 (1990) 1003-1015.

[33] W. Kim, J. Lee, Collection efficiency model based on boundary-layer characteristics for cyclones, AIChE J. 43 (1997) 2446-2455.

[34] M.B. Ray, A.C. Hoffmann, R.S. Postma, Performance of different analytical methods in evaluating grade efficiency of centrifugal separators, J. Aerosol Sci. 31 (2000) 563-581.

[35] C. Shephered, C. Lapple, Flow pattern and pressure drop in cyclone dust collectors, Ind. Eng. Chem. 31 (1939) 972-984.

[36] C. Stairmand, Pressure drop in cyclone separators, Engineering, 168 (1949) 409-412.

[37] J. Casal, J.M. Martinez-Benet, Better way to calculate cyclone pressure drop, Chem. Eng. 90 (1983) 99-100.

[38] R.M. Alexander, Fundamentals of cyclone design and operation, Proc. Aust. Inst. Mining Met. 152 (1949) 203.

[39] P. Patterson, R. Munz, Gas and particle flow patterns in cyclones at room and elevated temperatures, Can. J. Chem. Eng. 74 (1996) 213-221.

[40] W. Barth, L. Leineweber, Beurteilung und auslegung von zyklonabscheidern, Staub, 24 (1964) 41-55.

[41] P. Meissner, F. Löffler, Zur Berechnung des Strömungsfeldes im Zyklonabscheider, Chem-Ing-Technik. 50 (1978) 471-471.

[42] E. Muschelknautz, K. Brunner, Untersuchungen an zyklonen, Chem-Ing-Technik. 39 (1967) 531-538.

[43] D.L. Iozia, D. Leith, Effect of cyclone dimensions on gas flow pattern and collection efficiency, Aerosol Sci. Technol. 10 (1989) 491-500.

[44] H. Mothes, F. Löffler, Zur Berechnung der Partikelabscheidung in Zyklonen (A model for particle separation in cyclones), Chem. Eng. Process. 18 (1984) 323-331.

[45] S. Obermair, C. Gutschi, J. Woisetschläger, G. Staudinger, Flow pattern and agglomeration in the dust outlet of a gas cyclone investigated by phase doppler anemometry, Powder Technol. 156 (2005) 34-42.

[46] J. Gimbun, T. Chuah, T. S. Choong, A. Fakhru'l-Razi, A CFD study on the prediction of cyclone collection efficiency, Int. J. Comput. Meth. Eng. Sci. Mech. 6 (2005) 161-168.

[47] K.-Y. Kuo, C.-J. Tsai, On the theory of particle cutoff diameter and collection efficiency of cyclones, Aerosol Air Qual. Res. 1 (2001) 47-56.

[48] A. Gil, L. M. Romeo, C. Cortes, Effect of the solid loading on a PFBC cyclone with pneumatic extraction of solids, Chem. Eng. Technol. 25 (2002) 407-415.

[49] F.L.S. Fassani, L. Goldstein Jr, A study of the effect of high inlet solids loading on a cyclone separator pressure drop and collection efficiency Powder Technol. 107 (2000) 60-65.

[50] S. Kang, T. Kwon, S. D. Kim, Hydrodynamic characteristics of cyclone reactors, Powder Technol. 58 (1989) 211-220.

[51] S. Yuu, T. Jotaki, Y. Tomita, K. Yoshida, The reduction of pressure drop due to dust loading in a conventional cyclone, Chem. Eng. Sci. 33 (1978) 1573-1580.

[52] J. Derksen, S. Sundaresan, H. Van Den Akker, Simulation of mass-loading effects in gas-solid cyclone separators, Powder Technol. 163 (2006) 59-68.

[53] F. Qian, Z. Huang, G. Chen, M. Zhang, Numerical study of the separation characteristics in a cyclone of different inlet particle concentrations, Comput. Chem. Eng. 31 (2007) 1111-1122.